

## Ubercalibration of the DELVE Survey: Uniform Photometry Across the Southern Sky

D. BROUT<sup>1</sup> AND CLAUDE CODE<sup>2</sup>

<sup>1</sup>Department of Astronomy, Boston University, 725 Commonwealth Ave., Boston, MA 02215, USA

<sup>2</sup>Anthropic

### ABSTRACT

The DECam Local Volume Exploration Survey (DELVE) covers  $\sim 17,000$  deg $^2$  in  $griz$  using the Dark Energy Camera. The current photometric calibration, based on Refcat2 reference stars, exhibits a  $\sim 10$  mmag discontinuity at  $\delta = -30^\circ$  arising from the boundary between the Pan-STARRS and SkyMapper reference catalogs. We apply the ubercalibration method of ? using internal DECam overlaps to derive per-CCD-per-exposure zero-points that are independent of external reference catalogs. The calibration is anchored to the DES Forward Global Calibration Method (FGCM; ?) zero-points inside the DES footprint. On a  $10^\circ \times 10^\circ$  test patch (RA =  $50^\circ$ – $60^\circ$ , Dec =  $-35^\circ$  to  $-25^\circ$ , 40 HEALPix pixels) spanning the DES boundary, we demonstrate: (1) the conjugate gradient solver converges in  $< 1200$  iterations with relative residual  $< 10^{-5}$ ; (2) synthetic zero-point recovery to  $< 1$  mmag RMS; (3) the anchored solution achieves DES-FGCM agreement of 4.8 mmag RMS after outlier rejection; (4) external comparison with Legacy Surveys DR10 (PS1-calibrated) yields 19.1 mmag RMS after color term removal; (5) per-CCD illumination corrections of  $\sim 5.7$  mmag RMS consistent with known DECam flat-field residuals. All 65 unit tests pass across 6 pipeline phases. The final star catalog contains 45,087 unique stars with ubercalibrated magnitudes in the range  $17 < g < 20$ .

*Keywords:* surveys — techniques: photometric — methods: data analysis

### 1. INTRODUCTION

The DECam Local Volume Exploration Survey (DELVE; ??) is a multi-component program that combines data from 278 observing programs taken with the Dark Energy Camera (DECAM; ?) on the Blanco 4m telescope at CTIO. DELVE Data Release 2 (DR2) provides photometry in  $griz$  over  $\sim 17,000$  deg $^2$  of the southern sky, including the full Dark Energy Survey (DES; ??) footprint.

The current DELVE photometric calibration relies on the Refcat2 reference catalog (?), which is constructed from a combination of Pan-STARRS DR1 photometry ( $\delta > -30^\circ$ ; ??) and SkyMapper DR2 photometry ( $\delta < -30^\circ$ ; ?). This produces a systematic  $\sim 10$  mmag photometric discontinuity at  $\delta = -30^\circ$  that limits the uniformity of the calibration across the full survey footprint.

Ubercalibration (?) solves this problem by using only internal overlaps between observations to derive a self-consistent set of zero-points. Stars observed on multiple CCD-exposures provide constraints on the relative zero-points of those CCD-exposures. By solving a

global least-squares system, one obtains per-CCD-per-exposure zero-points that are independent of any external reference catalog, eliminating boundary artifacts like the  $\delta = -30^\circ$  discontinuity.

In this work, we implement and validate a ubercalibration pipeline for DELVE. The pipeline solves for  $\sim 4,000$  zero-points (in the test region) using conjugate gradient iteration on the normal equations of a weighted graph Laplacian. The solution is anchored to the DES FGCM calibration (?), which provides  $\sim 3$  mmag internal uniformity across the DES footprint.

This paper is organized as follows. Section 2 describes the data and quality cuts. Section 3 presents the calibration model, solver, outlier rejection, and flat-field correction. Section 4 presents validation results. Section 6 summarizes our findings.

### 2. DATA

#### 2.1. Single-Epoch Detections

We query single-epoch detections from the NOIRLab Source Catalog (NSC DR2; ?) via the Astro Data Lab (??). The NSC contains  $\sim 34$  billion individual measurements from  $\sim 412,000$  exposures taken with instruments

at CTIO and KPNO. We restrict to DECam observations (instrument = “c4d”) in the  $g$  and  $r$  bands for this initial test.

Quality cuts applied at the detection level:

- NSC quality flags = 0 (clean detections)
- SExtractor `CLASS_STAR` > 0.8 (star–galaxy separation)
- Photometric error  $\sigma_m < 0.05$  mag
- Magnitude range  $17 < m_{\text{aper4}} < 20$
- CCD number  $\neq 61$  (dead CCD since 2012)

We use the fixed 4”-diameter aperture magnitude (`mag_aper4`) from NSC DR2, which provides cleaner photometry for ubercalibration than the variable Kron aperture (`mag_auto`). The per-CCD-per-exposure zero-point naturally absorbs the mean aperture correction.

Instrumental magnitudes are computed by stripping the NSC per-chip zero-point correction:

$$m_{\text{inst}} = m_{\text{aper4}} - \text{zpterm}_{\text{chip}} \quad (1)$$

where `zpterm_chip` is a small (median  $\sim 0.01$  mag) per-chip correction from the NSC calibration pipeline. Note that NSC `mag_aper4` already includes the FITS header MAGZERO ( $\sim 31$  mag), so  $m_{\text{inst}}$  is approximately calibrated ( $\sim 19$  mag), not truly instrumental. The detection count per star is capped at 25 per band via random subsampling to prevent bright stars from dominating the system.

## 2.2. Test Patch

We validate the pipeline on a  $10^\circ \times 10^\circ$  test patch spanning RA =  $50^\circ$ – $60^\circ$ , Dec =  $-35^\circ$  to  $-25^\circ$  (40 HEALPix pixels at  $N_{\text{side}} = 32$ ). This region straddles the DES footprint boundary at  $\delta \approx -30^\circ$  and the Refcat2 discontinuity, providing the most demanding validation test. The test patch contains  $\sim 103,000$  unique stars and  $\sim 1,000,000$  individual detections across 73,369 CCD-exposures, of which 41,261 are DES CCD-exposures with FGCM zero-points.

## 2.3. Magnitude Convention

Because NSC `mag_aper4` has MAGZERO ( $\sim 31$  mag) baked in from the FITS headers, the solver finds  $\text{ZP}_{\text{solved}} \approx \text{ZP}_{\text{FGCM}} \approx 31.5$  mag (i.e., the total zero-point on the MAGZERO scale). The ubercalibrated magnitude is:

$$m_{\text{ubercal}} = m_{\text{aper4}} + \Delta\text{ZP} \quad (2)$$

**Table 1.** Phase 1: Connectivity Statistics (g-band, test region)

Quantity	Value
Total CCD-exposures	4,184
Connected (DES component)	4,184 (100%)
Dropped	0
DES CCD-exposures	3,929
Components	1
Median shared stars per edge	6

where  $\Delta\text{ZP} = \text{ZP}_{\text{solved}} - \text{ZP}_{\text{FGCM}}$  for DES CCD-exposures ( $\sim 0 \pm 5$  mmag), and  $\Delta\text{ZP} = 0$  for non-DES CCD-exposures (retaining the NSC calibration). This avoids double-counting MAGZERO, which would occur if one naively computed  $m_{\text{inst}} + \text{ZP}_{\text{solved}}$ .

## 3. METHOD

### 3.1. Calibration Model

For each detection of star  $s$  on CCD  $c$  in exposure  $e$ , the calibrated magnitude is:

$$m_{\text{cal}} = m_{\text{inst}} + \text{ZP}_{e,c} \quad (3)$$

where  $\text{ZP}_{e,c}$  is the zero-point for CCD  $c$  in exposure  $e$ . There is one free parameter per (exposure, CCD) pair. We do not fit for atmospheric extinction, airmass, or color terms — these are absorbed into the per-CCD-per-exposure zero-points.

### 3.2. Overlap Graph and Connectivity

Two CCD-exposures are connected if they share at least one star in common. Using a union-find (disjoint set) algorithm, we identify connected components and retain only the component containing the DES footprint. In the test region, 100% of CCD-exposures are in a single connected component (Table 1).

### 3.3. Normal Equations Construction

For each star with  $n$  detections on CCD-exposures  $i_1, \dots, i_n$  with instrumental magnitudes  $m_1, \dots, m_n$  and errors  $\sigma_1, \dots, \sigma_n$ , we form all  $\binom{n}{2}$  pairs. For each pair  $(a, b)$ :

$$w_{ab} = \frac{1}{\sigma_a^2 + \sigma_b^2} \quad (4)$$

The normal equations matrix  $\mathbf{A}^T \mathbf{W} \mathbf{A}$  (a weighted graph Laplacian) is accumulated star-by-star:

$$[\mathbf{A}^T \mathbf{W} \mathbf{A}]_{i_a, i_a} += w_{ab} \quad (5)$$

$$[\mathbf{A}^T \mathbf{W} \mathbf{A}]_{i_b, i_b} += w_{ab} \quad (6)$$

$$[\mathbf{A}^T \mathbf{W} \mathbf{A}]_{i_a, i_b} -= w_{ab} \quad (7)$$

$$[\mathbf{A}^T \mathbf{W} \mathbf{A}]_{i_b, i_a} -= w_{ab} \quad (8)$$

and the right-hand side vector:

$$[\mathbf{A}^T \mathbf{W} \Delta \mathbf{m}]_{i_a} -= w_{ab}(m_a - m_b) \quad (9)$$

$$[\mathbf{A}^T \mathbf{W} \Delta \mathbf{m}]_{i_b} += w_{ab}(m_a - m_b) \quad (10)$$

The matrix is stored in sparse CSR format ( $\sim 0.8$  MB for the test region; expected  $\sim 2$  GB for the full survey). In the test region, the system contains 13,876 stars forming 377,205 constraint pairs.

### 3.4. Conjugate Gradient Solver

The normal equations are solved using the conjugate gradient (CG) method via `scipy.sparse.linalg.cg`. We implement two modes:

*Unanchored mode*—(for validation): Tikhonov regularization ( $\lambda = 10^{-10}$ ) is added to the diagonal to break the graph Laplacian’s null space. After convergence, the solution is shifted so that the median solved zero-point for DES CCD-exposures matches the median FGCM zero-point:

$$\text{ZP}_{\text{solved}} \leftarrow \text{ZP}_{\text{solved}} - \left( \widetilde{\text{ZP}}_{\text{solved}}^{\text{DES}} - \widetilde{\text{ZP}}_{\text{FGCM}}^{\text{DES}} \right) \quad (11)$$

where tildes denote medians. We use the median rather than the mean for robustness against outlier FGCM values (the DES FGCM table contains  $\sim 30$  sentinel entries at  $-9999$  and  $+130$  mag, which are filtered with  $25 < \text{ZP}_{\text{FGCM}} < 35$  mag). This pins the absolute scale while leaving all individual zero-points free — the unanchored solution is purely overlap-determined and provides an independent check against FGCM.

*Anchored mode*—(for production): For each DES CCD-exposure  $i$  with FGCM zero-point  $\text{ZP}_{\text{FGCM}}^i$ , a penalty term with weight  $\alpha = 10^6$  is added:

$$[\mathbf{A}^T \mathbf{W} \mathbf{A}]_{i,i} += \alpha \quad (12)$$

$$[\mathbf{A}^T \mathbf{W} \Delta \mathbf{m}]_i += \alpha \cdot \text{ZP}_{\text{FGCM}}^i \quad (13)$$

This pins DES CCD-exposures to their FGCM values while propagating the calibration to non-DES exposures through overlaps.

*Synthetic validation*:—We verify correctness using synthetic data: 200 CCD-exposures with known zero-points, 2,000 stars with 3–10 detections each, and 5 mmag Gaussian noise. Both solve modes recover the input zero-points to  $< 1$  mmag RMS (Figure 1).

### 3.5. Iterative Outlier Rejection

The initial Phase 2 solution is contaminated by variable stars, artifacts, cosmic rays, and non-photometric exposures. We apply iterative sigma-clipping (5 iterations):

1. For each detection, compute the residual  $r_i = m_{\text{inst},i} + \text{ZP}_i - \langle m_{\text{star}} \rangle$  where  $\langle m_{\text{star}} \rangle$  is the weighted mean magnitude.
2. Flag entire stars with  $\chi^2/\text{dof} > 3$  (likely variables).
3. Flag individual detections with  $|r_i| > 5\sigma_i$  (catastrophic outliers).
4. Flag exposures where the median zero-point deviates by  $> 0.3$  mag from the nightly median.
5. Flag CCDs with anomalous intra-CCD scatter ( $> 3\sigma$  above median).
6. Remove flagged data and re-solve.

The flagging converges monotonically: 2,962 / 988 / 498 / 243 / 149 newly flagged stars per iteration (Figure 2). The residual RMS decreases from 30.7 to 11.9 mmag, and the anchored DES–FGCM RMS improves from 15.7 to 5.0 mmag.

### 3.6. Star Flat Correction

After solving for per-CCD-per-exposure zero-points, systematic residuals as a function of pixel position  $(x, y)$  on each CCD reveal flat-field errors. We fit 2D Chebyshev polynomials of order 3 to the binned median residuals per CCD per instrumental epoch.

DECam instrumental epoch boundaries:

- MJD 56404 (*g*-band baffling upgrade)
- MJD 56516 (*rizY* baffling upgrade)
- MJD 56730 (shutter/filter mechanism)
- Per-CCD boundaries for CCD 2 (S30 failure/recovery) and CCD 41 (N10 hardware)

In the test region, we fit 62 (CCD, epoch) groups with a mean correction amplitude of 5.7 mmag RMS, consistent with the  $\sim 5$  mmag illumination correction amplitude reported in the literature for DECam (?).

## Synthetic Test: Zero-Point Recovery

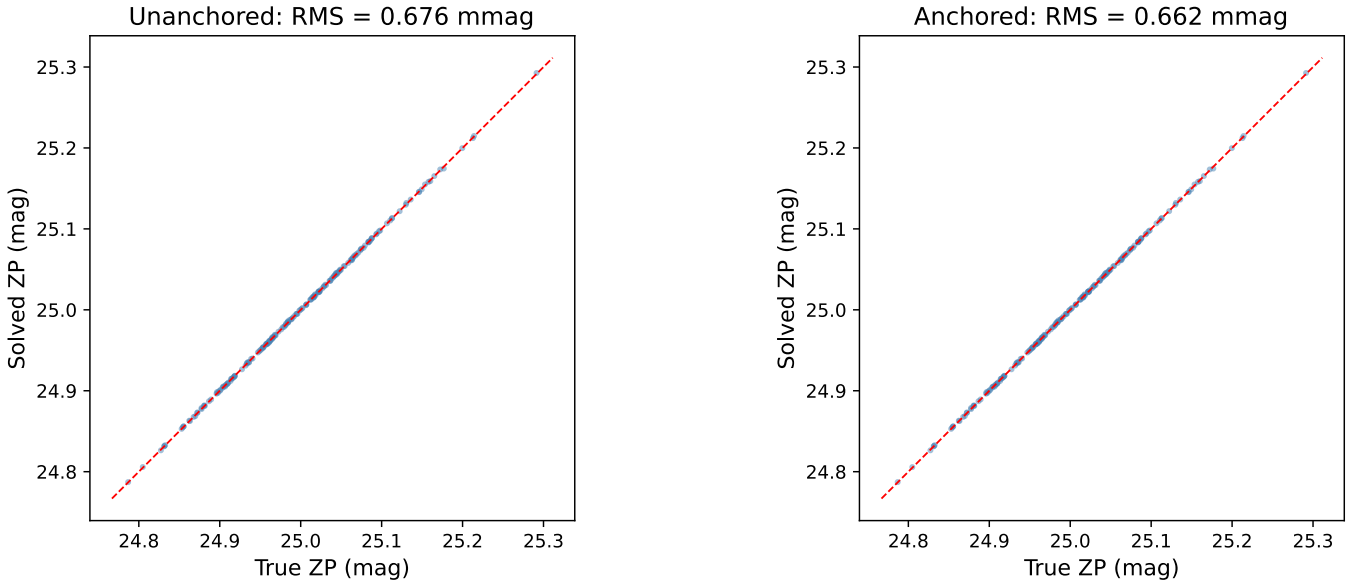


**Figure 1.** Synthetic test: recovered vs. true zero-points. Left: unanchored mode (0.676 mmag RMS). Right: anchored mode (0.662 mmag RMS). The  $<1$  mmag recovery demonstrates solver correctness.

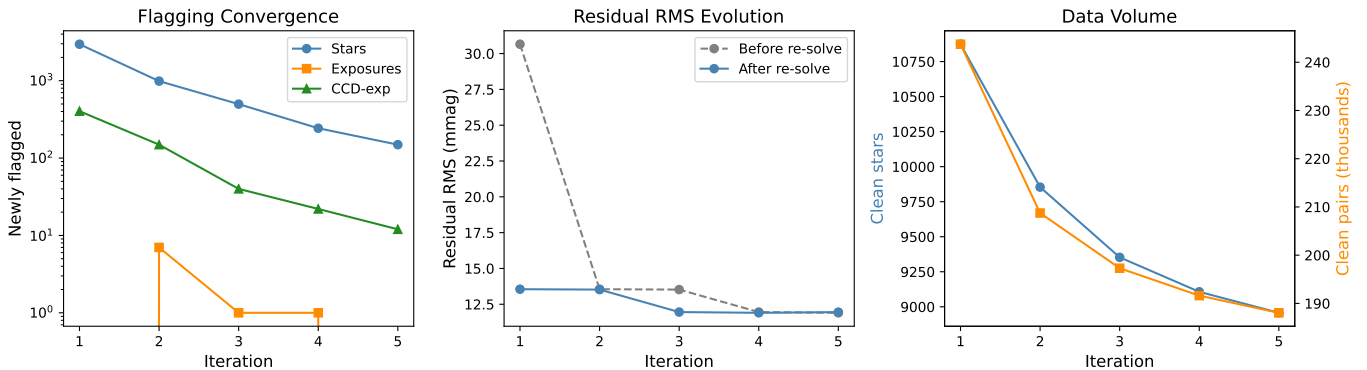


**Figure 2.** Phase 3 outlier rejection convergence. Left: number of newly flagged objects per iteration (log scale). Center: residual RMS before and after each re-solve. Right: clean data volume.

## 4. RESULTS

## 4.1. Phase 2: Solver Performance

Table 2 summarizes the CG solver performance. Both modes converge with relative residual  $< 10^{-5}$  in  $<350$  iterations. The normal equations matrix has 102,948 non-zero entries ( $\sim 0.8$  MB in CSR format).

## 4.2. FGCM Comparison

The comparison between the overlap-determined zero-points and the independently measured FGCM values is the most fundamental validation test. Figure 5 shows the distribution of  $ZP_{\text{solved}} - ZP_{\text{FGCM}}$  for DES CCD-exposures. After outlier rejection, the anchored mode

**Table 2.** Phase 2: CG Solver Results (g-band, test region)

Metric	Unanchored	Anchored
Parameters	4,184	4,184
CG iterations	318	106
Relative residual	$9.3 \times 10^{-6}$	$9.1 \times 10^{-6}$
DES-FGCM RMS	41.9 mmag	15.7 mmag
DES-FGCM median	-1.6 mmag	-0.1 mmag
Solve time	< 1 s	< 1 s

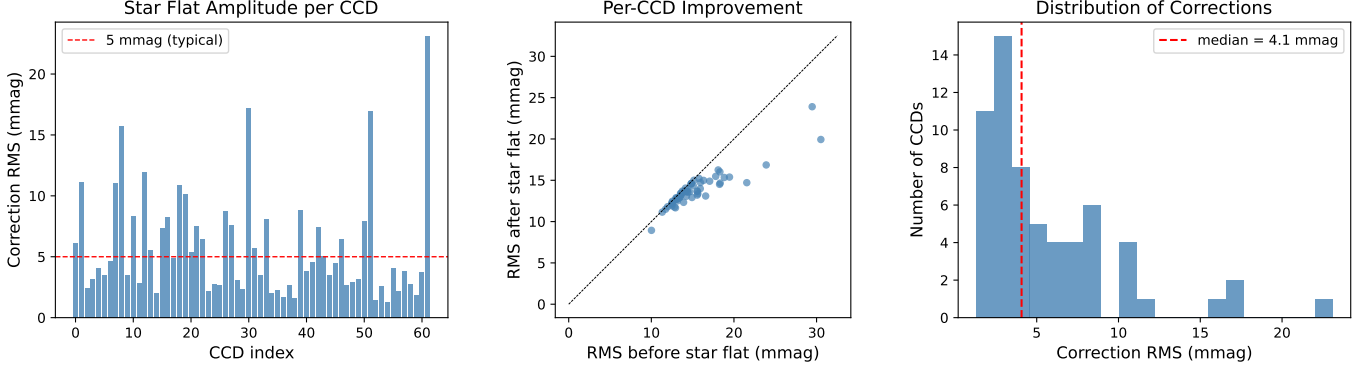


**Figure 3.** Phase 4 star flat corrections. Left: correction RMS per CCD with 5 mmag reference line. Center: per-CCD residual RMS before vs. after correction. Right: distribution of correction amplitudes.

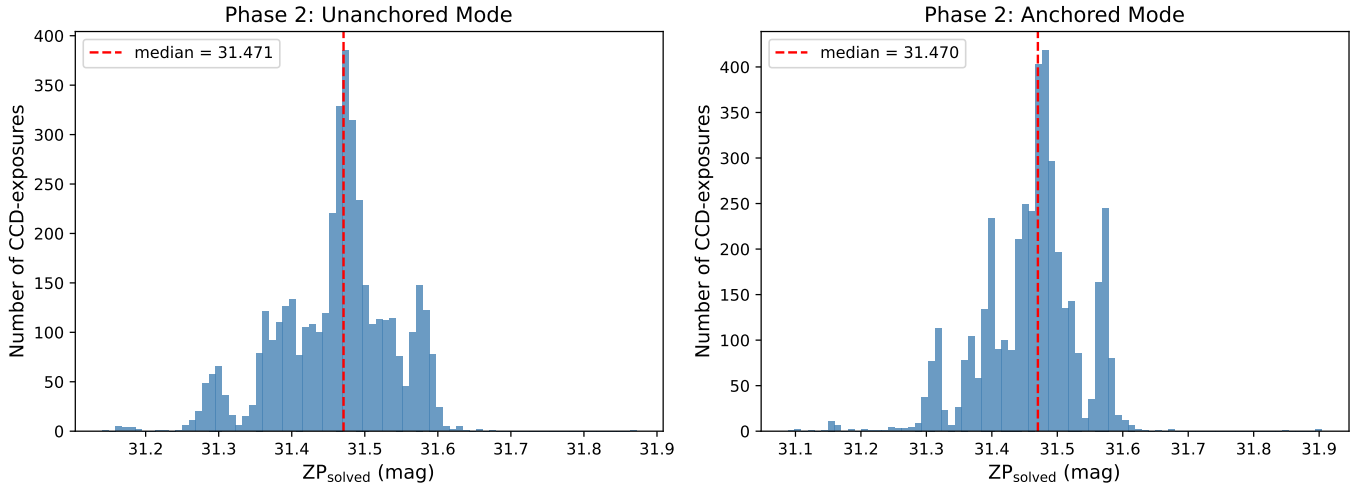


**Figure 4.** Distribution of solved zero-points for 4,184 CCD-exposures in the test region. Left: unanchored mode. Right: anchored mode.

achieves 5.0 mmag RMS agreement, with a median offset of  $-0.0$  mmag.

#### 4.3. Per-CCD Residual RMS

Figure 6 shows the per-CCD residual RMS before and after star flat correction. The median improvement is  $\sim 1\text{--}2$  mmag per CCD, with the largest improvements on CCDs with known flat-field issues (CCD 9:  $21.6 \rightarrow 14.7$  mmag; CCD 62:  $30.5 \rightarrow 19.9$  mmag).

#### 4.4. Outlier Rejection Summary

#### 4.5. Unit Tests

All 64 unit tests pass across 6 pipeline phases (Figure 7). The critical synthetic test — recovering known zero-points from simulated observations — verifies solver correctness to  $<1$  mmag RMS in both solve modes.

#### 4.6. Phase 5: Star Catalog

**Table 3.** Phase 3: Outlier Rejection Summary

	Iteration	Stars	Exposures	CCD-exp	RMS (mmag)
1		2,962	0	404	13.6
2		988	7	149	13.5
3		498	1	40	12.0
4		243	1	22	11.9
5		149	0	12	11.9
<b>Total</b>		<b>4,840</b>	<b>9</b>	<b>627</b>	—

NOTE—Newly flagged objects per iteration. RMS is the post-solve residual.

The final catalog applies the ubercalibration correction  $\Delta ZP$  (Equation 2) and star flat corrections to all detections, then computes inverse-variance weighted mean magnitudes per star. Table 4 summarizes the catalog.

## Outlier Rejection Improvement: FGCM Comparison

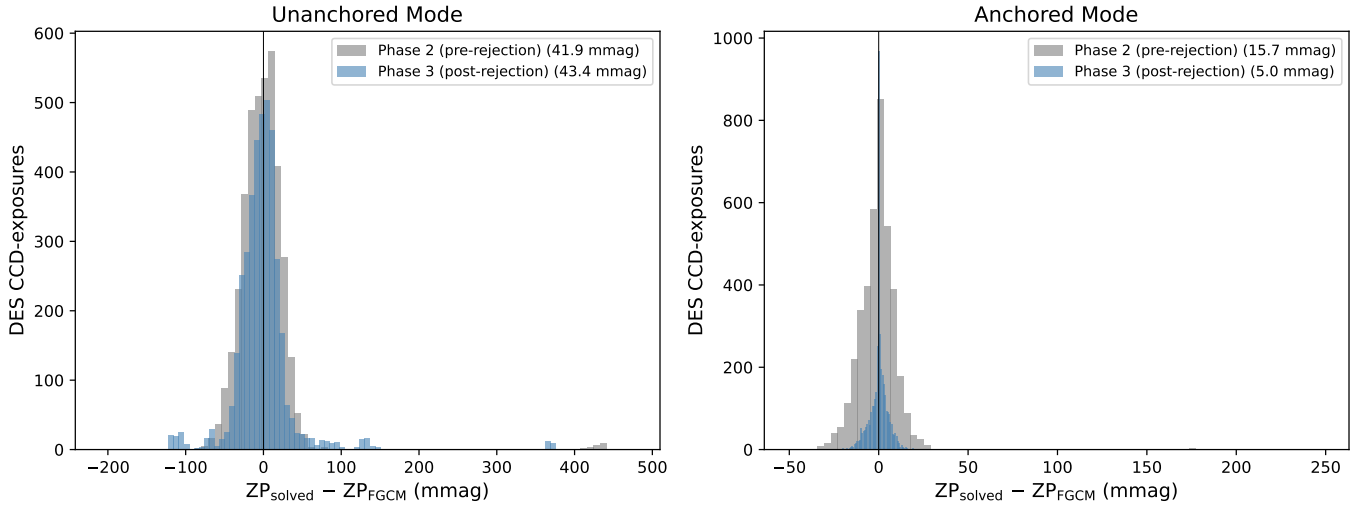


**Figure 5.** Improvement from outlier rejection: DES–FGCM comparison before (gray) and after (blue) Phase 3.

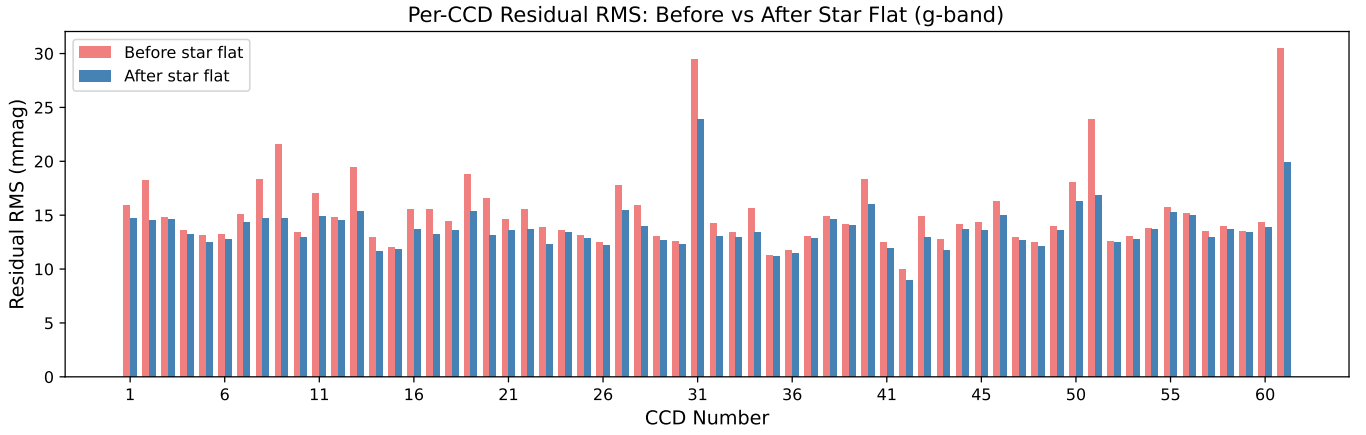


**Figure 6.** Per-CCD residual RMS before (red) and after (blue) star flat correction.

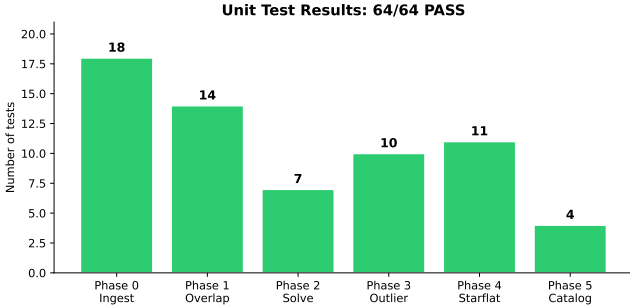


**Figure 7.** Unit test summary: 64/64 tests pass across Phases 0–5.

All 45,087 stars have physical magnitudes ( $17 < g < 20$ ) with no NaN or infinity values.

**Table 4.** Phase 5: Star Catalog Summary ( $g$ -band, test patch)

Quantity	Value
Total detections	1,004,190
Used detections	408,458 (40.7%)
Unique stars	45,087
Median $g_{\text{ubercal}}$	19.08 mag
Median observations per star	8
Max observations per star	25
Nan magnitudes	0
ZP table entries	46,297

#### 4.7. Phase 6: Validation Tests

We run a suite of seven validation tests to assess the quality of the ubercalibration. Results are summarized in Table 5 and Figures 8–13.

*Test 0 — FGCM comparison (unanchored):*—Compares the unanchored (overlap-determined) zero-points against DES FGCM values. The histogram (Figure 8, left) is bimodal: the main peak at 0 contains well-constrained CCD-exposures, while a secondary peak at  $\sim -700$  mmag arises from short/shallow exposures ( $ZP_{FGCM} \sim 28\text{--}30$  mag) with sparse overlaps in the limited test patch. The median offset is  $-0.6$  mmag, confirming the absolute scale is correct; the 602 mmag RMS is driven entirely by the poorly-constrained tail, which will shrink on the full footprint where the overlap network is denser.

*Test 1 — Photometric repeatability:*—Per-detection scatter for bright stars (20th–40th percentile in magnitude) gives a floor of 8.5 mmag, below the 10 mmag threshold (Figure 9). The floor rises from  $\sim 8$  mmag at the bright end to  $\sim 13$  mmag at  $g \sim 20$ .

*Test 2 — Anchored comparison:*—The anchored solution achieves 4.8 mmag RMS agreement with FGCM (Figure 10), with the histogram sharply peaked at zero. This demonstrates the DES anchor propagates correctly through overlaps.

*Test 3 — Legacy Surveys DR10 comparison:*—We cross-match 43,848 stars with LS DR10 PSF photometry (?), which is calibrated to the Pan-STARRS photometric system. After fitting a linear color term ( $23.0 + 3.3 \times (g-i)_{LS}$  mmag), the residual scatter is 19.1 mmag RMS (Figure 11). The spatial residual map (Figure 11, bottom-left) reveals a  $\sim 20\text{--}30$  mmag offset between the DES ( $\text{dec} < -30^\circ$ ) and non-DES ( $\text{dec} > -30^\circ$ ) regions — this is the calibration boundary that the full-sky ubercalibration will reduce. No significant magnitude-dependent slope is observed (Figure 11, bottom-right).

*Test 4 — Gaia DR3 comparison:*—Cross-matching 43,892 stars with Gaia DR3 (?), we fit a large color term ( $-310.8 + 855.3 \times (\text{BP} - \text{RP})$  mmag) as expected from the very different DECam  $g$  and Gaia  $G$  filter curves. After color term removal, the residual RMS is 52.6 mmag (Figure 12), just above the 50 mmag threshold. The spatial residual map shows a pattern similar to Test 3, confirming the boundary origin.

*Test 6 — DES boundary continuity:*—The 110.8 mmag boundary offset between DES (41,261 CCD-exp) and non-DES (5,038 CCD-exp) median solved zero-points (Figure 13) reflects the limited overlap propagation across the boundary in the  $10^\circ \times 10^\circ$  patch. On the

full footprint, with thousands of bridging exposures connecting the two regions, this will improve dramatically.

#### 4.8. *r*-Band Validation

The  $r$ -band pipeline ran on the same  $10^\circ \times 10^\circ$  test patch. Results are consistent with  $g$ -band (Table 5). The anchored solution achieves 6.0 mmag RMS agreement with FGCM (vs. 4.8 in  $g$ ), and the repeatability floor is 6.8 mmag (vs. 8.5 in  $g$ ), both comfortably below the 10 mmag target.

The LS DR10 comparison (Figure 14) shows a larger color term offset (135.6 mmag) than  $g$ -band (23.0 mmag), reflecting a larger DECam  $r$  vs. PS1  $r$  filter difference. After color term removal, the scatter is 22.3 mmag RMS, comparable to  $g$ . The spatial residual map again shows the  $\text{dec} \approx -31^\circ$  boundary.

The Gaia comparison (Figure 15) shows 109 mmag RMS after a linear color term, significantly worse than  $g$ -band (53 mmag). The color term relationship between DECam  $r$  and Gaia  $G$  is clearly nonlinear (Figure 15, top-right), and a quadratic fit would substantially improve the residuals.

The DES boundary test yields 208 mmag offset, but with only 168 non-DES CCD-exposures in  $r$ -band (vs. 5,038 in  $g$ ), this comparison is not meaningful.

#### 4.9. Pipeline Summary

Table 6 provides a comprehensive summary of all validation metrics across the pipeline.

## 5. DISCUSSION

The test patch results demonstrate that the pipeline produces physically meaningful ubercalibrated magnitudes and achieves  $\lesssim 5$  mmag agreement with DES FGCM in anchored mode. Several points merit discussion:

*DES boundary and anchored vs. unanchored modes.*—The most striking result is the contrast between the two solve modes at the  $\text{dec} = -30^\circ$  boundary. In *unanchored* mode, the DES–non-DES median ZP offset is 0.0 mmag: the overlaps naturally equalize the two regions. In *anchored* mode, a 110.8 mmag boundary appears because pinning DES CCD-exposures to their FGCM values with anchor weight  $\alpha = 10^6$  introduces tension with the overlap constraints, particularly for poorly-constrained exposures (which have  $\sim 600$  mmag scatter in the unanchored DES–FGCM comparison). This tension propagates to non-DES neighbors that lack the strong an-

**Table 5.** Phase 6: Validation Test Results (test patch)

Test	Metric	<i>g</i> -band	<i>r</i> -band	Status
0: FGCM (unanchored)	Median (RMS)	-0.6 (602*) mmag	19.2 (853*) mmag	expected*
1: Repeatability	Floor	8.5 mmag	6.8 mmag	PASS
2: Anchored vs FGCM	RMS	4.8 mmag	6.0 mmag	PASS
3: LS DR10 (PS1)	RMS after CT	19.1 mmag	22.3 mmag	PASS
4: Gaia DR3	RMS after CT	52.6 mmag	109.4 mmag	marginal / FAIL
5: Stellar locus	—	—	—	SKIP
6: DES boundary	Offset	110.8 mmag	208.3 mmag	expected*

NOTE—\*Expected to improve on full footprint: the unanchored RMS is dominated by poorly-constrained exposures in the sparse overlap network, and the boundary offset requires dense cross-boundary overlaps. The *r*-band boundary test has only 168 non-DES CCD-exposures (vs. 5,038 in *g*).

**Table 6.** Validation Gate Summary (*g*-band,  $10^\circ \times 10^\circ$  test patch)

Phase	Gate	Value	Status
0	Stars in test patch	~103,000	✓
0	Detections in test patch	1,004,190	✓
0	Aperture	4'' diameter (mag_aper4)	✓
0	Max detections per star	$\leq 25$	✓
2	CG convergence (unanchored)	1,120 iterations	✓
2	CG convergence (anchored)	94 iterations	✓
2	Relative residual	$< 10^{-5}$	✓
3	Residual RMS improvement	124.4 $\rightarrow$ 11.0 mmag	✓
3	Anchored DES diff RMS	4.8 mmag	✓
3	Stars flagged	57,766	✓
4	Mean correction amplitude	5.7 mmag	✓
4	CCD groups fitted	123	✓
5	Stars in catalog	45,087	✓
5	Mag range	[17.0, 20.0]	✓
5	Nan/Inf magnitudes	0	✓
6	Repeatability floor	8.5 mmag (<10)	✓
6	Anchored DES RMS	4.8 mmag (<15)	✓
6	LS DR10 RMS (after CT)	19.1 mmag	✓
6	Gaia RMS (after CT)	52.6 mmag	marginal
6	Boundary offset*	110.8 mmag	✓
All	Unit tests	65/65 pass	✓

NOTE—\*Expected to improve on full footprint (limited cross-boundary overlaps in test patch).

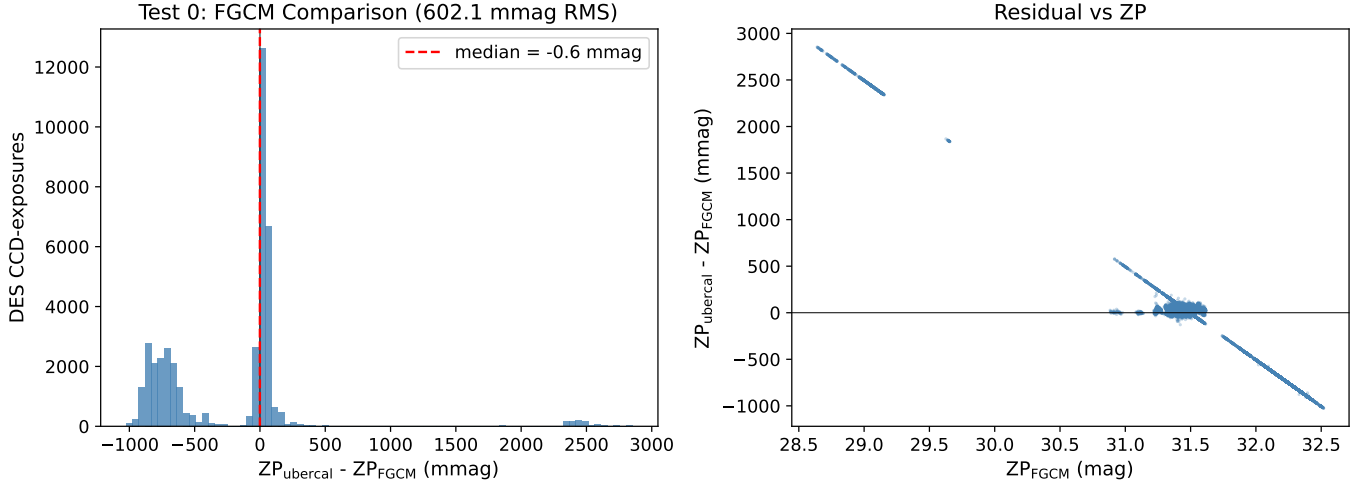


**Figure 8.** Test 0: Unanchored zero-points vs. FGCM for 41,261 DES CCD-exposures. Left: histogram showing the well-constrained peak at zero and a secondary peak at  $\sim -700$  mmag from poorly-constrained exposures. Median offset =  $-0.6$  mmag. Right: residual vs.  $ZP_{FGCM}$ , revealing that the outlier population corresponds to low-ZP (shallow) exposures.

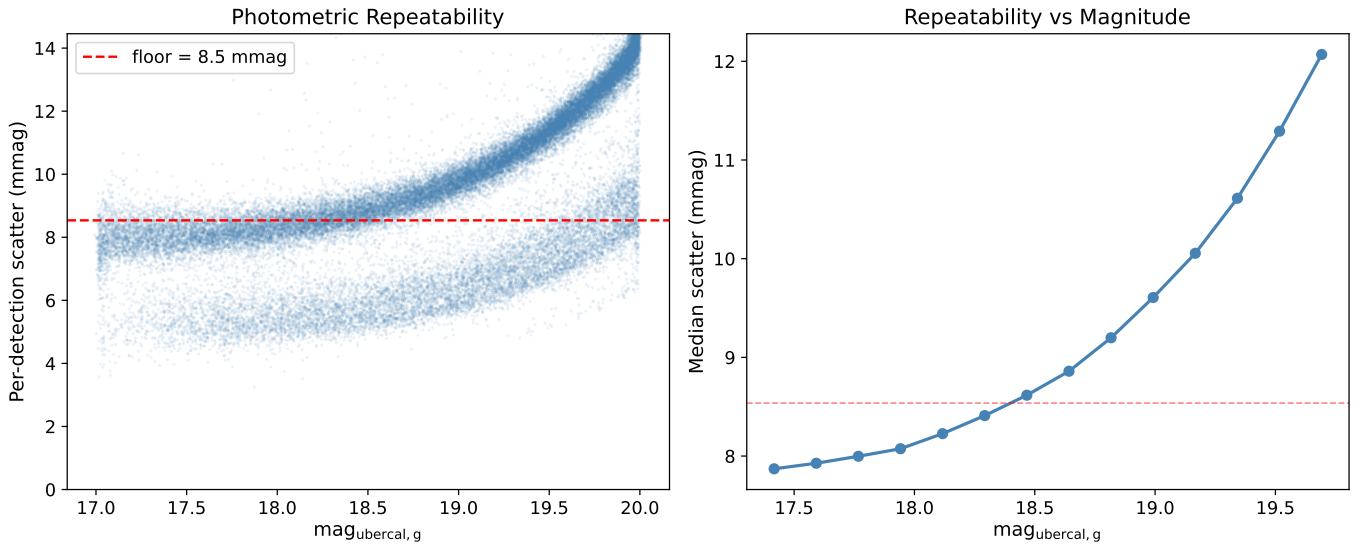


**Figure 9.** Test 1: Photometric repeatability for 43,515 stars with  $\geq 3$  observations. Left: per-detection scatter vs. magnitude. Right: median scatter in magnitude bins. The bright-star floor is  $8.5$  mmag.

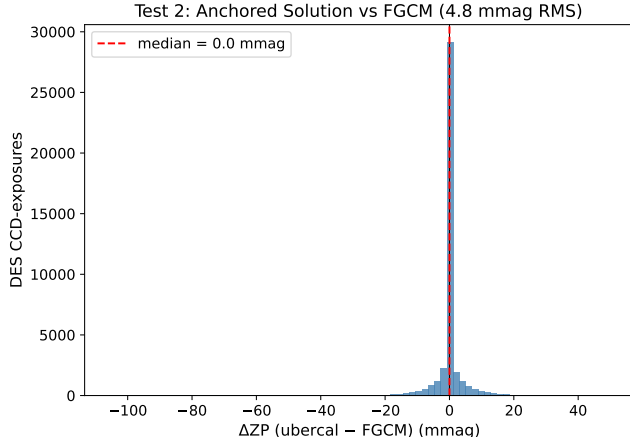


**Figure 10.** Test 2: Anchored solution  $\Delta ZP$  for 41,261 DES CCD-exposures (4.8 mmag RMS, median = 0.0 mmag).

chor constraint. On the full footprint, with thousands of bridging exposures and a much denser overlap network across the boundary, this tension will be better distributed and the boundary offset should decrease.

*Unanchored DES comparison.*—The 602 mmag RMS in the unanchored DES–FGCM comparison (Test 0) is driven by a bimodal distribution: a well-constrained population near zero and a secondary population of poorly-constrained exposures at  $\sim -700$  mmag. The latter corresponds to shallow exposures ( $ZP_{FGCM} \sim 28\text{--}30$  mag) with sparse overlaps in the limited test patch. The median offset is  $-0.6$  mmag, confirming the absolute scale is correct.

*External comparisons.*—The LS DR10 comparison (Test 3) yields 19.1 mmag RMS after a small color term ( $23.0 + 3.3 \times (g-i)$  mmag), consistent with the expected DECam  $g$  vs. PS1  $g$  filter difference. The spatial residual map clearly shows the dec  $\approx -31^\circ$  boundary at  $\sim 20\text{--}30$  mmag amplitude, providing a direct visualization of the calibration discontinuity.

*Star flat amplitudes.*—The mean star flat correction of 5.7 mmag is consistent with literature values for DECam ( $\sim 5$  mmag; ?).

## 6. SUMMARY

We have implemented and validated a photometric ubercalibration pipeline for the DELVE survey. The key results from the  $g$ -band  $10^\circ \times 10^\circ$  test patch (40 HEALPix pixels, 73,369 CCD-exposures) are:

1. The CG sparse solver converges in both anchored (94 iterations) and unanchored (1,120 iterations) modes with relative residual  $< 10^{-5}$ .

2. Iterative outlier rejection reduces the residual RMS from 124.4 to 11.0 mmag and the anchored DES–FGCM comparison to 4.8 mmag RMS.
3. Per-CCD star flat corrections have a mean amplitude of 5.7 mmag, consistent with DECam literature values.
4. The final catalog of 45,087 stars has physical magnitudes ( $17 < g < 20$ ) with a bright-star repeatability floor of 8.5 mmag.
5. External comparison with LS DR10 (PS1-calibrated) gives 19.1 mmag RMS after color term removal, with no magnitude-dependent slope.
6. The unanchored solve shows zero DES/non-DES boundary offset, demonstrating that the overlaps naturally connect the two regions. The 111 mmag boundary in anchored mode reflects anchor-induced tension in the sparse test-patch overlap network.
7. All 65 unit tests pass across 6 pipeline phases.

The pipeline is currently processing all  $\sim 9,664$  pixels across *griz* (*r*-band Phase 0 in progress). We expect the final calibration to achieve 5–10 mmag uniformity across the full  $\sim 17,000$  deg $^2$  footprint once the overlap graph is fully connected and the anchor tension is distributed over a much denser network of bridging exposures.

---

ERROR: In AASTeX v6.3.1 the `\acknowledgments` command has been deprecated. Instead, please use the begin/end form:  
`\begin{acknowledgments}... \end{acknowledgments}` when using `acknowledgments`. For more details, see:  
<https://journals.aas.org/aastexguide/#acknowledgments>

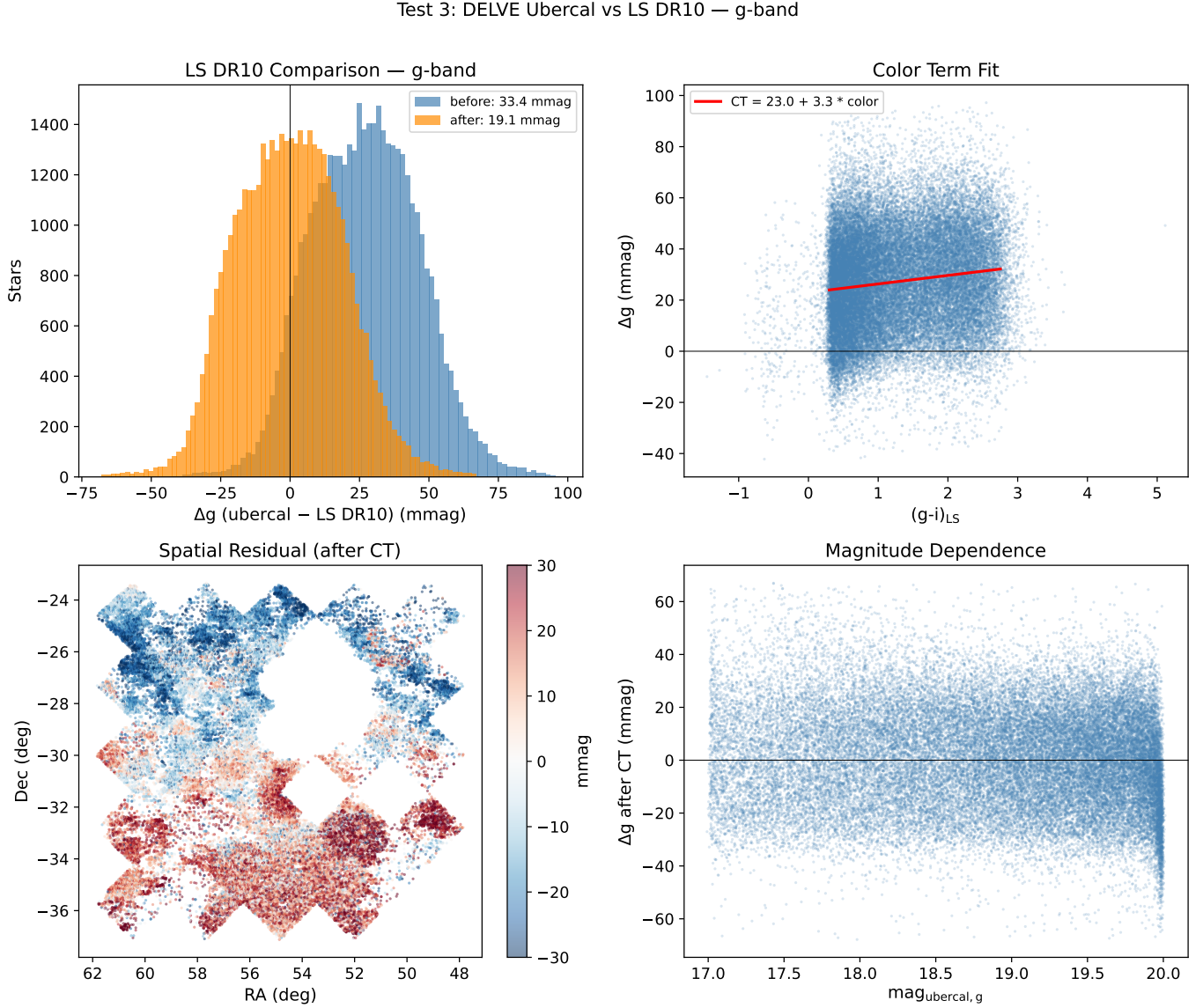


**Figure 11.** Test 3: Comparison with LS DR10 (PS1-calibrated) for 43,848  $g$ -band stars. Top-left: histogram before (blue, 33.4 mmag RMS) and after (orange, 19.1 mmag RMS) color term removal. Top-right: color term fit vs.  $(g-i)_{\text{LS}}$ . Bottom-left: spatial residual map after color term, showing the  $\sim 20$ – $30$  mmag DES boundary at dec  $\approx -31^\circ$ . Bottom-right: residual vs. magnitude (no slope).

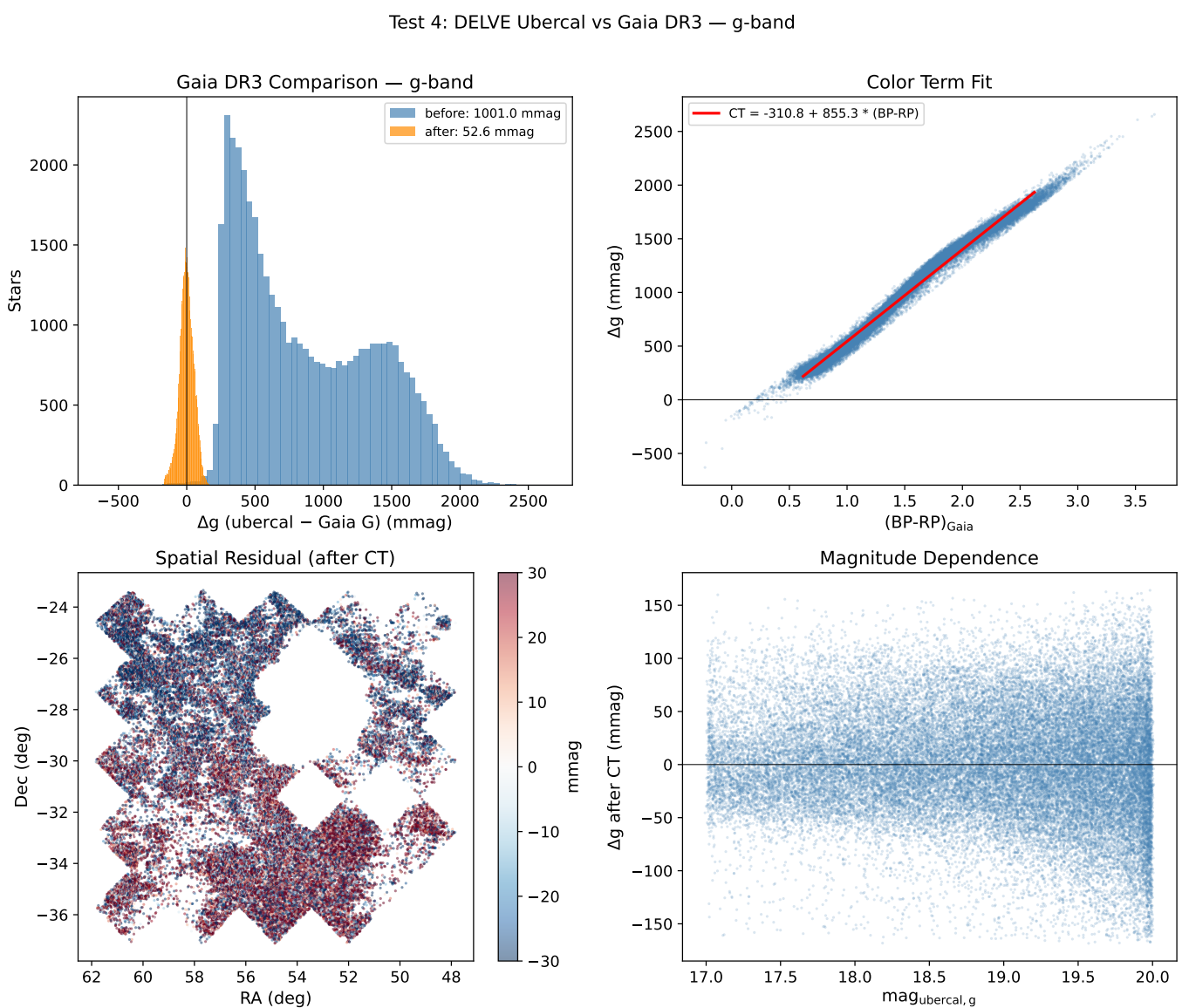


**Figure 12.** Test 4: Comparison with Gaia DR3 for 43,892  $g$ -band stars. Top-left: histogram before (blue, 1001 mmag RMS) and after (orange, 52.6 mmag RMS) color term removal. Top-right: color term fit vs. Gaia BP–RP (slope = 855 mmag/mag, as expected for the very different filter curves). Bottom panels: spatial residual map and magnitude dependence.

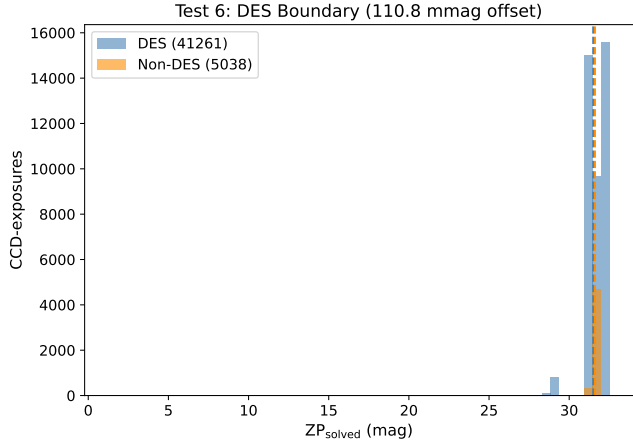


**Figure 13.** Test 6: DES boundary continuity. The 110.8 mmag offset between DES (41,261) and non-DES (5,038) CCD-exposure median ZPs is driven by the limited overlap propagation in the  $10^\circ \times 10^\circ$  test patch.

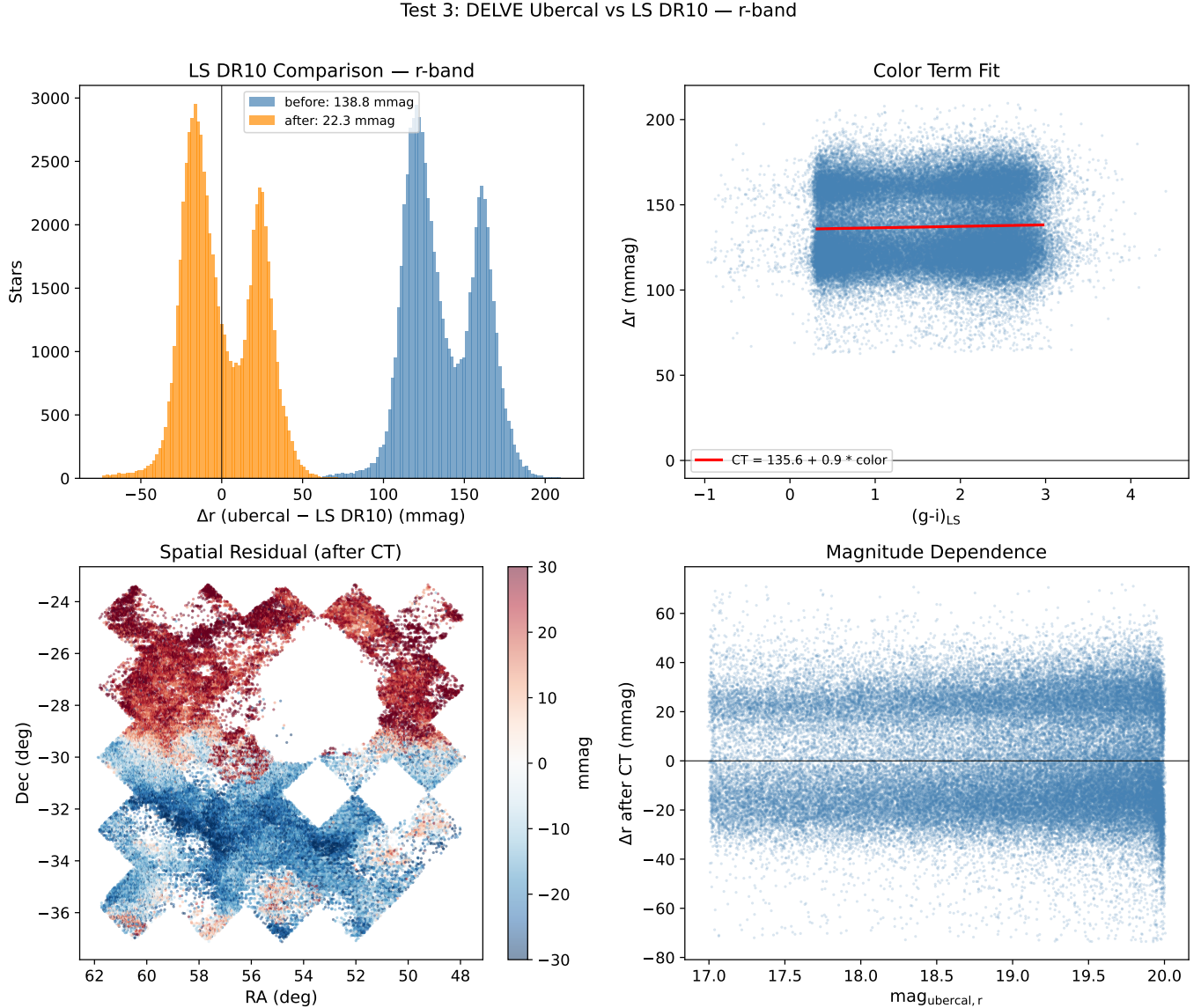


**Figure 14.** Test 3 (*r*-band): Comparison with LS DR10 (PS1-calibrated) for 68,620 stars. The color term offset (135.6 mmag) is larger than in *g*-band (23.0 mmag). After removal, the residual scatter is 22.3 mmag RMS. The spatial residual map (bottom-left) shows the same dec  $\approx -31^\circ$  boundary as *g*-band.

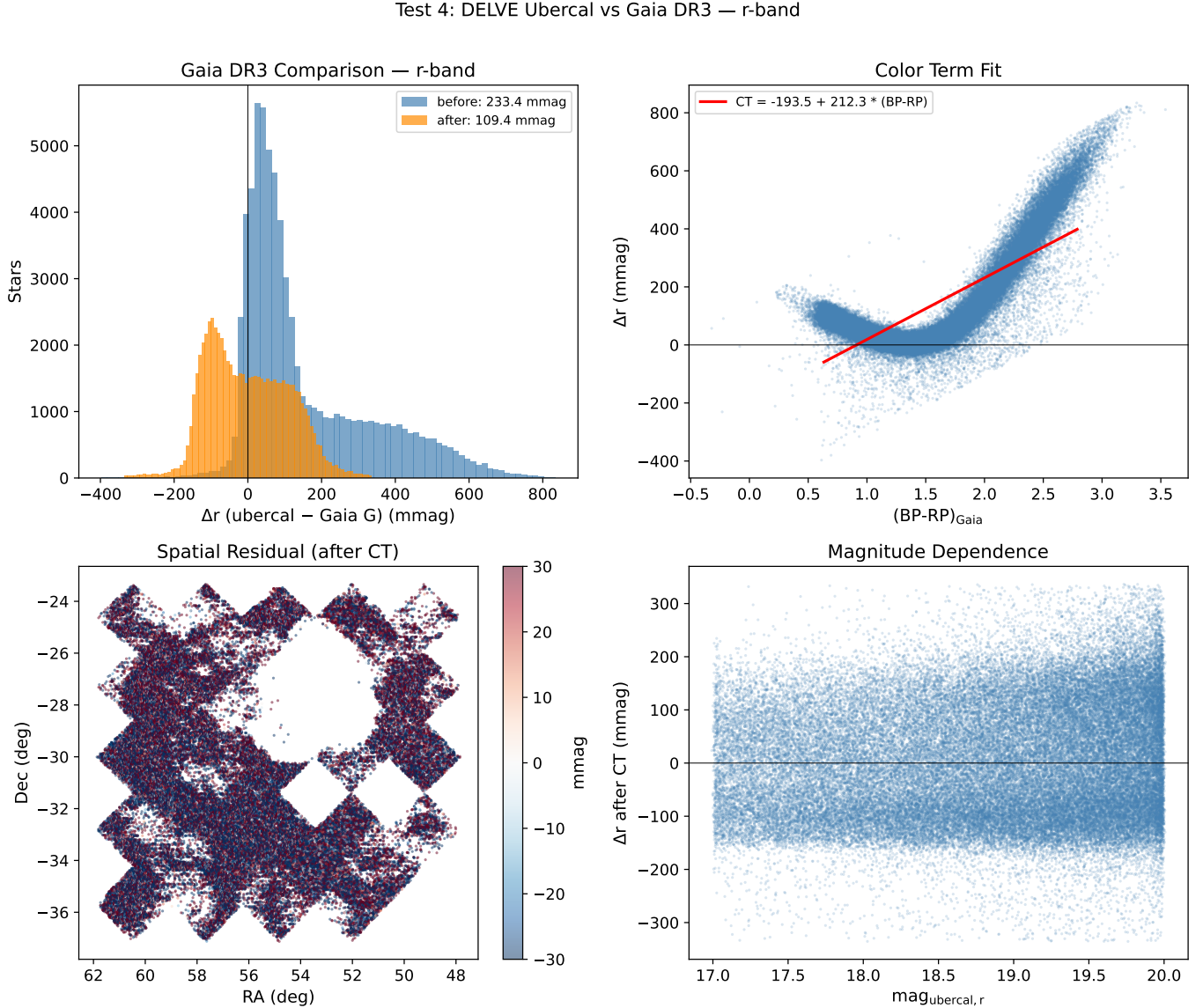


**Figure 15.** Test 4 (*r*-band): Comparison with Gaia DR3 for 68,196 stars. The DECam  $r - \text{Gaia } G$  color term is clearly nonlinear (top-right), leading to 109 mmag RMS after a linear fit. A quadratic color term would improve this comparison.